Metal Oligo-yne Polymers: Electronic Structures of $[-(L)_nMC{\equiv}CRC{\equiv}C-]_x$ Polymers

Gilles Frapper*,† and Miklos Kertesz*

Department of Chemistry, Georgetown University, Washington, D.C. 20057-2222

Received July 28, 1992

The electronic structures of poly-ynes containing transition metals, $-[-(L)_nMC{\equiv}CRC{\equiv}C-]_x-$ (L = e.g. PR_3, CO, H; n = 0, 2, 3, 4; M = e.g. Mo, Fe, Rh, Pt, Hg; R = e.g. C≡C, *p*-C_6H_4) have been studied using the extended Hückel theory. Their optical properties depend on several factors: (i) the size and the nature of the oligo-yne bridging ligand, C≡CRC≡C, (ii) the coordination of the metal, n, and finally the metal itself. Bonding properties are accounted for by the usual 16 and 18 electron rules. The d^8 square-planar configuration (e.g. M = Pt, n = 2) presents a larger conduction bandwidth than the d^6 octahedral one (e.g. M = Fe, n = 4), offering a better chance for electrical conduction. The HOCO is delocalized, for both n = 2 and n = 4 coordinations.

Since the synthesis of poly-ynes containing transition metals of group 10 in the main chain by Sonogashira, Takahashi, Hagihara, and their co-workers,[1] the physical properties exhibited by these polymers have attracted much attention. Both physicists and chemists speak with enthusiasm of nonlinear optical behavior[2-4] and of liquid-crystalline properties[5,6] of this family of compounds. Recently, different synthetic approaches have been developed, extending the data concerning polymeric species[2,7-10] and their related oligomeric forms[11-18] for group 8-10 transition metals, and for a large class of π-conjugated bridging ligands. In Figure 1, we show a limited number of such polymers and molecular species which we study in this paper.

Because of the introduction of the metal-ligand groups, $M(L)_n$, into the poly-yne backbone, these materials offer versatility that cannot be matched by the conventional π-conjugated organic polymers (e.g. poly(thiophene), polyacetylene). For example, changing the nature of the ligands may improve the solubility[19] of the polymer without significantly altering the electrical properties, which are derived from the π-system of the carbon backbone.

One of the interesting features of these one-dimensional organometallic polymers **1a**, **2a** and **3a**, doped and undoped, is the phenomenon of electrical conductivity due to the presence of metal-carbon σ-bonds and the carbon π-system in the backbone. The experimental values[20,21] for the band gap are around 3 eV and classify these polymers as weak conductors in their undoped state. Doping is expected to increase the conductivity, just like that of any other conjugated polymer.[22] There is only one indication in the experimental literature to that effect so far.[20]

The study of the electronic band structures of this family of compounds may help to rationalize the effects that several factors have in the conduction properties: the nature of the transition metal atom M and its coordination, the conjugation of the π-system for the bridging ligand, C≡CRC≡C, and the nature of the ligand field, $(L)_n$.

We are going to use throughout this paper tight-binding solid state and molecular calculations of the extended Hückel type,[23] with parameters described in the Appendix. We shall designate polymers of the type **1a**, **2a**, and **3a** as metal oligo-yne polymers, MOP's.[24]

Influence of the Metal Coordination on the Electronic Properties

The MOP's synthesized so far can be classified in two structural classes, as shown in Figure 1: the local coordination environment at each transition metal is, locally, for the first class, octahedral for d^6 metals (e.g. M = Fe^{II} in **1a**,[7] M = Rh^{III} in **2a**,[8,9]), and for the second one, square-planar for d^8 metals (e.g. M = Pt^{II} in **3a**[1]), in accordance to the well-known 16 and 18 electron rules for these structural configurations.[25] The corresponding oligo-ynes

† Permanent address: Laboratoire de Chimie du Solide et Inorganique Moléculaire, URA 1495 (ex 254), CNRS, Université de Rennes I, 35042 Rennes, France.

(1) (a) Sonogashira, K.; Takahashi, S.; Hagihara, N. *Macromolecules* **1977**, *10*, 879-880. (b) Takahashi, S.; Kariya, M.; Yatake, T.; Sonogashira, K.; Hagihara, N. *Macromolecules* **1978**, *11*, 1063-1066. (c) Takahashi, S.; Murata, E.; Sonogashira, K.; Hagihara, N. *J. Polym. Sci. Chem. Ed.* **1980**, *18*, 661-669. (d) Hagihara, N. J.; Sonogashira, K.; Takahashi, S. *Adv. Poly. Sci.* **1981**, *41*, 149-179 and references therein.

(2) Marder, T. B.; Lesley, G.; Yuan, Z.; Fyfe, H. B.; Chow, P.; Stringer, G.; Jobe, I. R.; Taylor, N. J.; Williams, I. D.; Kurtz, S. K. *ACS Symp. Ser.* **1991**, *No. 455*, 605-615.

(3) Porter, P. L.; Guha, S.; Kang, K.; Frazier, C. C. *Polymer* **1991**, *32*, 1756-1760.

(4) (a) Williams, D. J., Ed. *Nonlinear Optical Properties of Organic Molecules and Crystals*; ACS Symposium Series No. 233; American Chemical Society: Washington, DC, 1983. (b) Prasad, P. N.; Williams, D. J. *Introduction to Nonlinear Optical Effects in Molecules and Polymers*; Wiley-Interscience: New York, 1991. (b) Short review of metalla-enes and metalla-ynes: Chisholm, M. H. *Angew. Chem., Int. Ed. Engl.* **1991**, *30*, 673-674.

(5) Abe, A.; Kimura, N.; Tabata, S. *Macromolecules* **1991**, *24*, 6238-6243.

(6) Kaharu, T.; Matsubara, H.; Takahashi, S. *J. Mater. Chem.* **1991**, *1*, 145-146.

(7) Johnson, B. F. G.; Kakkar, A. K.; Khan, M. S.; Lewis, J. *J. Organomet. Chem.* **1991**, *409*, C12-C14.

(8) Davies, S. J.; Johnson, B. F. G.; Khan, M. S.; Lewis, J. *J. Chem. Soc., Chem. Commun.* **1991**, 187-188.

(9) Fyfe, H. B.; Mlekus, M.; Zargarian, D.; Taylor, N. J.; Marder, T. B. *J. Chem. Soc., Chem. Commun.* **1991**, 188-190.

(10) Khan, M. S.; Davies, S. J.; Kakkar, A. K.; Schwartz, D.; Lin, B.; Johnson, B. F. G.; Lewis, J. *J. Organomet. Chem.* **1992**, *424*, 87-97.

(11) Chow, P.; Zargarian, D.; Taylor, N. J.; Marder, T. B. *J. Chem. Soc., Chem. Commun.* **1989**, 1545-1547.

(12) Field, L. D.; George, A. V.; Hambley, T. W.; Malouf, E. Y.; Young, D. J. *J. Chem. Soc., Chem. Commun.* **1990**, 931-933.

(13) Davies, S. J.; Johnson, B. F. G.; Lewis, J.; Khan, M. S. *J. Organomet. Chem.* **1991**, *401*, C43-C45.

(14) Akita, M.; Terada, M.; Oyama, S.; Moro-oka, Y. *Organometallics* **1990**, *9*, 816-825.

(15) Onitsuka, K.; Ogawa, H.; Joh, T.; Takahashi, S.; Yamamoto, Y.; Yamazaki, H. *J. Chem. Soc., Dalton Trans.* **1991**, 1531-1536.

(16) Wong, A.; Kang, P. C. W.; Tagge, C. D.; Leon, D. R. *Organometallics* **1990**, *9*, 1992-1994.

(17) McDonald, R.; Sturge, K. C.; Hunter, A. D.; Shilliday, L. *Organometallics* **1992**, *11*, 900-907.

(18) Chukwu, R.; Hunter, A. D.; Santarsiero, B. D.; Bott, S. G.; Atwood, J. L.; Chassaignac, J. *Organometallics* **1992**, *11*, 589-597.

(19) Tolman, C. A. *Chem. Rev.* **1977**, *77*, 313-348.

(20) Dray, A. E.; Wittmann, F.; Friend, R. H.; Donald, A. M.; Khan, M. S.; Lewis, J.; Johnson, B. F. G. *Synth. Met.* **1991**, *41-43*, 871-874.

(21) Lewis, J.; Khan, M. S.; Kakkar, A. K.; Johnson, B. F. G.; Marder, T. B.; Fyfe, H. B.; Wittmann, F.; Friend, R. H.; Dray, A. E. *J. Organomet. Chem.* **1992**, *425*, 165-176.

(22) Skotheim, T., Ed. *Handbook of conducting Polymers*; Dekker: New York, 1986; Vols. 1-2.

(23) (a) Hoffmann, R. *J. Chem. Phys.* **1963**, *39*, 1397. (b) Hoffmann, R.; Lipscomb, W. N. *J. Chem. Phys.* **1962**, *37*, 2872.

(24) Capitaine, N. M.; Mathews, J.; Akapulco, J. *In my Village: My garden*; Washington, D.C., 1992. Private communication.

(25) For general discussions, see: Albright, T. A.; Burdett, J. K.; Whangbo, M. H. *Orbitals Interactions in Chemistry*; Wiley-Interscience: New York, 1981.

0020-1669/93/1332-0732$04.00/0

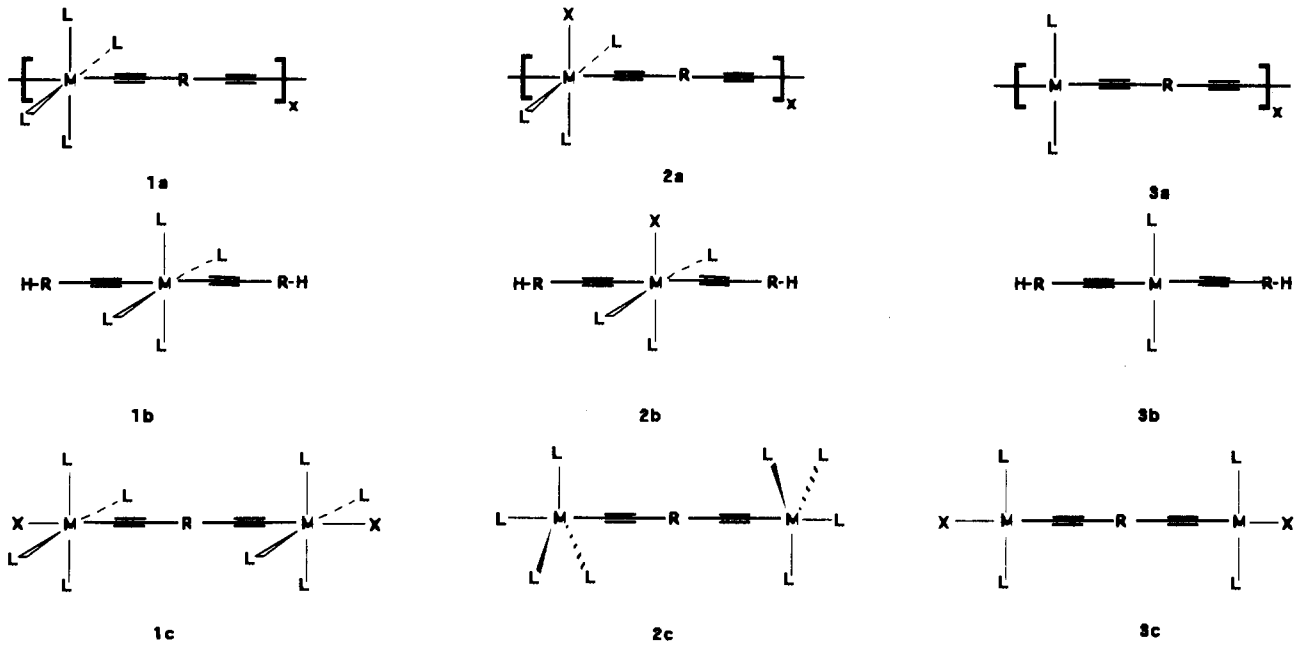

Figure 1. Structures of the metal oligo-yne polymers **1a**, **2a**, **3a** and their related oligomers **1b**, **1c**, **2b**, **2c**, **3b** and **3c**. M is the transition metal; X and L are one or two electrons ligands, respectively; R is none, C≡C, *p*-C_6H_4, C≡CC≡C, etc. **1a**, **1b**, **1c**: M = Fe^{II}, Ru^{II}, group 8; L = e.g. PBu_3, CO; X = e.g. Cl, SCN. **2a**, **2b**, **2c**: M = Co^{III}, Rh^{III}, group 9; L = e.g. PMe_3; X = e.g. H, $SnMe_3$. **3a**, **3b**, **3c**: M = Ni^{II}, Pd^{II}, Pt^{II}, group 10; L = e.g. PBu_3, $AsBu_3$; X = e.g. Cl, SCN.

1b,**c**, **2b**, and **3b**,**c**, which have the same electron counting and structural environment, follow this classification. On the other hand, the metal coordination of the dimetallic center oligo-yne **2c** (e.g. M = Rh^I) could be viewed as a trigonal bipyramid at each d^8 metal, with an 18 electron count.

To point out the principal characteristics of these two classes of MOP's, $-[-(L)_nMC{\equiv}CRC{\equiv}C-]_x-$, **1a** and **3a**, we are going to perform a fragmentation analysis on their respective monomers **1b** and **3b**, as described in Figure 2. Building up step by step these model compounds, our molecular approach should depict the frontier orbitals implicated in the valence (highest occupied) and conduction (lowest unoccupied) bands of the polymers under study. Calculations were performed on the $(L)_nM(C{\equiv}CRH)_2$ monomers, for M = Fe, L = PH_3, R = *p*-C_6H_4, C≡C, and *n* = 4 for **1b** and *n* = 2 for **3b**. Geometrical and atomic parameters, listed in the Appendix, are kept constant allowing a qualitative comparison of the effect of the different environments.

First of all, Figure 3 shows the principal orbital interactions between the metal M^{2+} with two and four phosphine ligands, called $(L)_2$ and $(L)_4$ during our discussion. The C_{2v} symmetry labels are chosen for clarity, because this is the symmetry of the final compounds **1b** and **3b** (see Figure 2). The right and left side of the interaction diagram are the two and four levels of the ligands implicated in the σ-interactions with the transition metal. Looking at the ML_2^{2+} fragment, what is happening? Two phosphine lone pairs, a_1 and b_1 in symmetry, interact with their symmetry match, M(s + $x^2 - y^2$) and M(x), respectively.

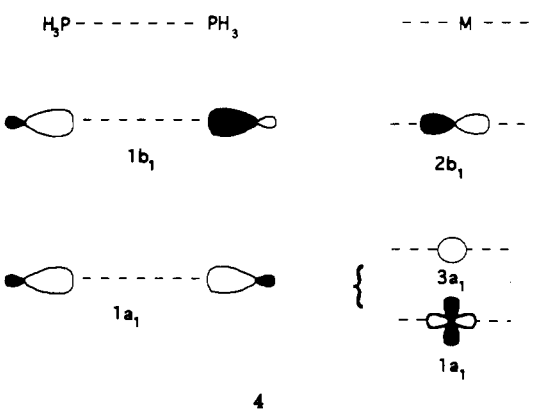

4

Two orbitals, mainly on P, Fe–P σ bonding, go down. By the same token, their antibonding combinations with a metal character go up. For the ML_4^{2+} fragment, the well-known interaction diagram is expected: Four phosphine lone pairs, $a_1 + (b_1, b_2) + a_1$ in symmetry, interact with their symmetry match, M(s), the degenerate orbitals M(x, y) and M($x^2 - y^2$), respectively.

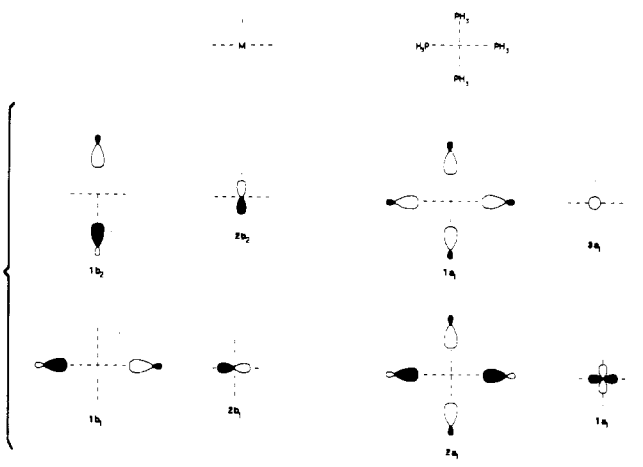

5

These Fe–P σ bonding orbitals go down in energy and their antibonding combinations go up. Both fragments have the d-π orbitals ((xz) and (yz), at −12.6 eV) interacting slightly with the phosphine p-π orbitals which are higher in energy (around −5 eV). These features show the weak π-acceptor and moderate σ-donor characters of the phosphine ligand. But the major change going from the ML_2^{2+} to the ML_4^{2+} fragments comes from the $2a_1$ and $2b_2$ orbitals which are mainly M($x^2 - y^2$) and M(y), respectively. Both are destablized by the two additional ligands due to the antibonding character of their interaction with the ligand lone pairs $2a_1$ and $1b_2$. A practical way to visualize this fact is to look at the composition of the d block for both fragments, going from 5 to 4 orbitals (see Figure 3).

Now, what happens when the metal–ligand fragment $[M(L)_n]^{2+}$ is connected with an oligo-yne chain $[HRC{\equiv}C\text{- - -}C{\equiv}CRH]^{2-}$? For brevity, we are going to describe the frontier orbitals of **1b** and **3b** monomers for R = *p*-C_6H_4. Figure

4 shows the principal orbital interactions between these two fragments, for $n = 2$ and 4. We can see than the σ_{M-C} bonding consist of the stabilizing interactions between the $1a_1$ and $2a_1$ yne orbitals with the mainly metal z^2 and z empty orbitals, respectively.

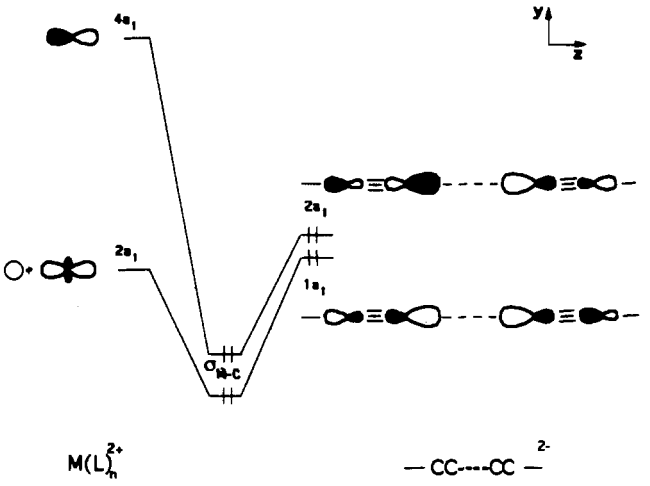

6

Since we are interested in this paper in the electrical properties, let us focus our attention on the highest occupied molecular orbital (HOMO) and the lowest unoccupied one (LUMO). Because of the introduction of the phenyl group in the oligo-yne fragment $[C_6H_5C{\equiv}C\text{- - -}C{\equiv}CC_6H_5]^{2-}$, the two oligo-yne-based π-systems, π_x and π_y, b_1 and b_2 in symmetry, are splitting in energy: $1b_2$ MO (at −12.5 eV) is higher in energy than $1b_1$ (at −13.0 eV), because this remains delocalized along the whole carbon skeleton. This filled π_y MO interactions with the M(yz) MO, giving a bonding π_{M-C} combination and an antibonding one, which becomes the HOMO (around −12.0 eV). Therefore, the main interactions between these orbitals are four-electron, destabilizing ones.

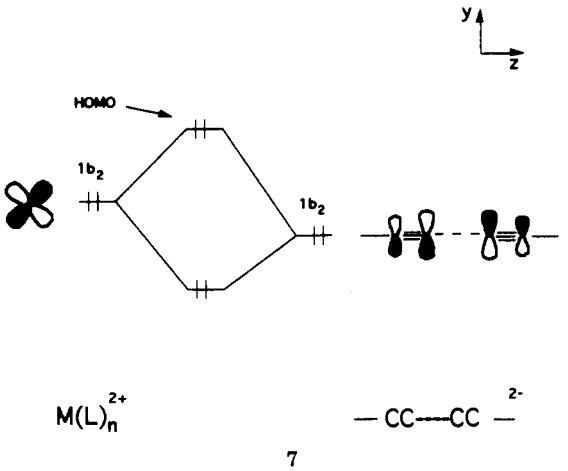

7

For both $ML_4(C{\equiv}CRH)_2$ (**1b**) and $ML_2(C{\equiv}CRH)_2$ (**3b**) monomers, the HOMO has, approximately, half-and-half metal–carbon character. Since the π^* carbon levels lie high above the filled metal-based orbitals, back-donation is weak.[26]

What about the LUMO? For monomer **3b**, the $2b_2$ and $3b_2$ π^* MO's split in energy, due to a bonding interaction coming from the M(y) $2b_2$ level, and to an antibonding interaction coming from the M(yz) $1b_2$ level.

(26) Theoretical study: (a) Kostić, N. M.; Fenske, R. F. *Organometallics* **1982**, *1*, 974–982. Experimental ones: (b) Beddoes, R. L., Bitcon, C.; Whiteley, M. W. *J. Organomet. Chem.* **1991**, *402*, 85–96. (c) Bruce, M. I.; Humphrey, M. G.; Snow, M. R.; Tiekink, E. R. T. *J. Organomet. Chem.* **1986**, *314*, 213–225.

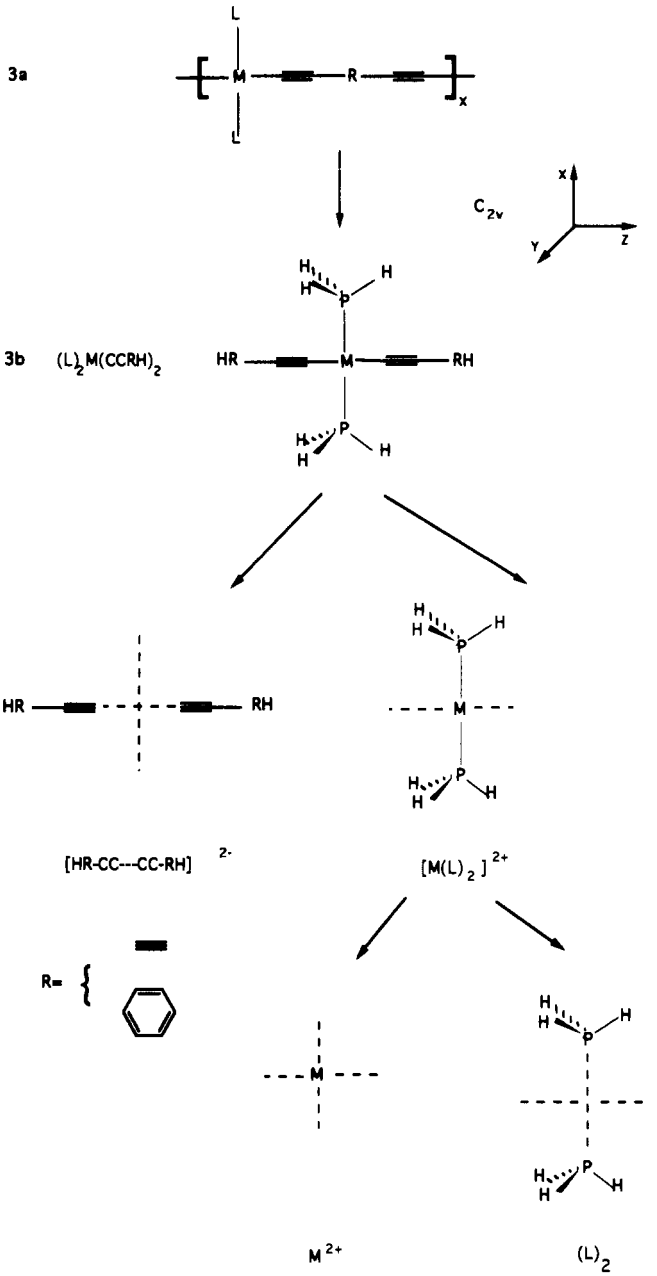

Figure 2. Fragmentation analysis of the $-[-(L)_2MC{\equiv}CRC{\equiv}C-]_x-$ polymer **3a** and derivatives. Similar modeling is performed for polymers **1a** and **2a**.

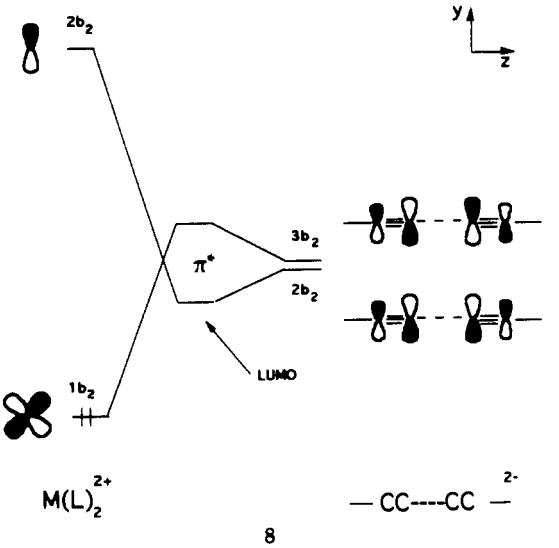

8

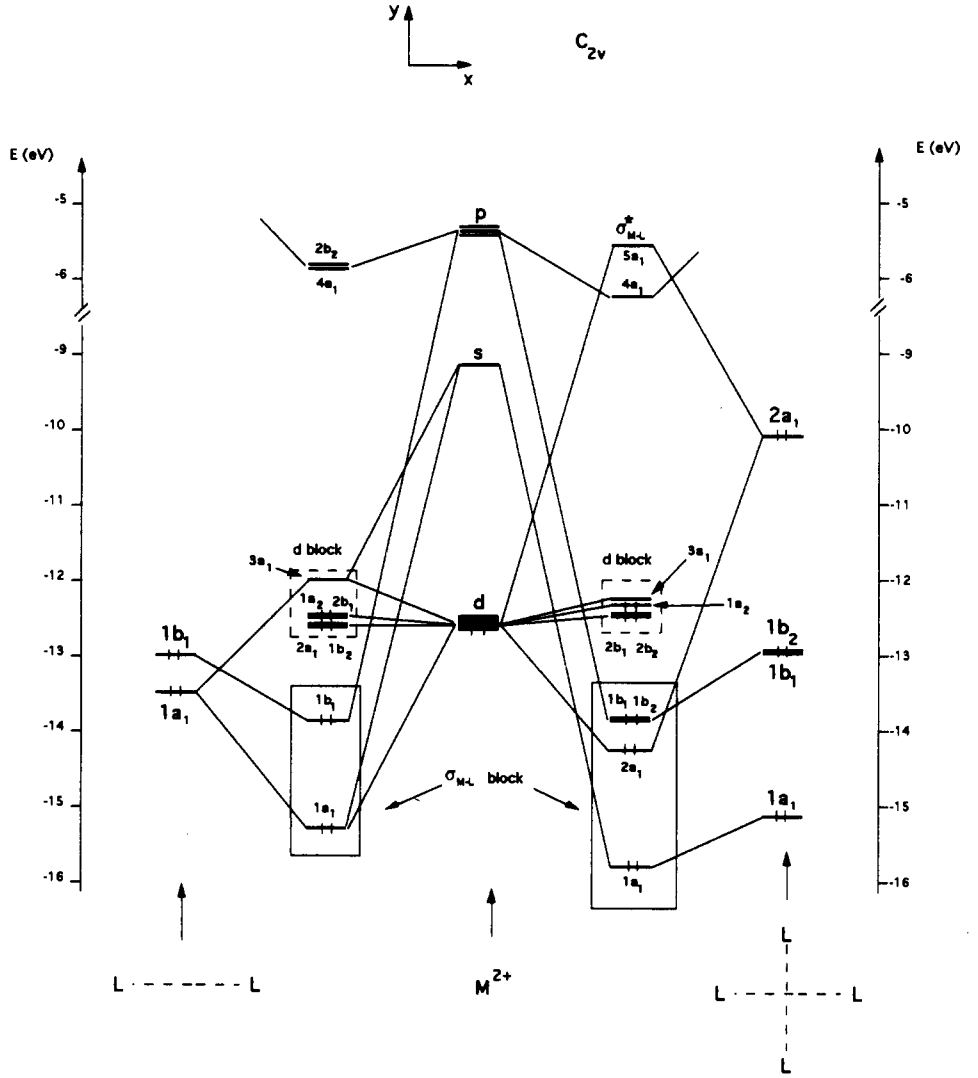

Figure 3. Interaction diagrams of $M(L)_n^{2+}$ (M = Fe; L = PH_3; n = 2, 4). On the left side and right side are the lone pair levels of $(L)_2$ and $(L)_4$, respectively. The levels of $M(L)_n^{2+}$ fragments are filled according to a d^8 metal, with n = 2, and a d^6 metal, with n = 4.

In contrast, for the monomer **1b**, both of these π^* carbon levels are destabilized by the antibonding contributions of the mainly $2b_2$ M(yz) and the $1b_2$ P(σ_{M-P}) molecular orbitals.

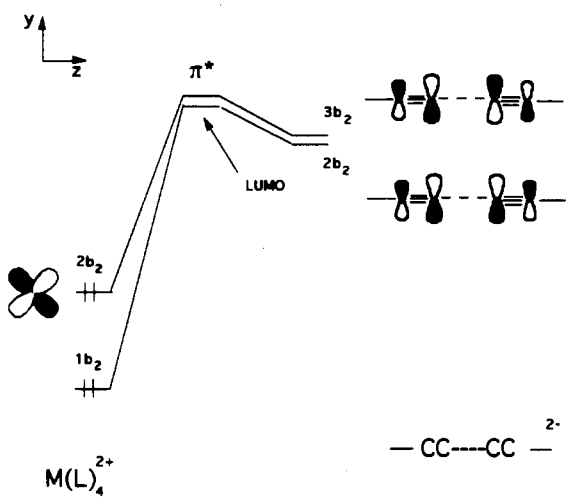

9

This simple feature indicates that going from the monomeric unit to the polymer, a greater dispersion of the conduction band (or bandwith) of the lowest unoccupied crystal orbital, LUCO, should be expected for the MOP **3a** as compared to **1a**.

Electronic Structure of the Infinite Poly-yne Metal Chains

We expect that going from the molecular compound to the infinite chain **1a**, **2a** and **3a**, the delocalization of the π-system along the carbon backbone and the metal groups will lead to a smaller band gap (see Table I). Going from **3b** to **3a** (with M = Pt, R = p-C_6H_4 and L = PH_3), the gap value decreases by 0.7 eV, while from **3c** (with X = Cl) to **3a**, the gap value decreases by 0.3 eV. In **3a**, the shape of the carbon chain is closer to **3c** than to **3b**: in **3b**, the metal–ligand fragment cuts the π-carbon system. A simple calculation on $HC{\equiv}CC_6H_4C{\equiv}CH$, **10**, shows that the LUMO energy of **3b** and **10** are the same; only the energy of the HOMO goes up, because of the participation of the d-π orbitals as described in **7**. These remarks are also valid for the poly-yne containing transition metal in coordination 6.

Let us now turn to the band structures for the $-[-(PH_3)_4FeC{\equiv}CC_6H_4C{\equiv}C-]_x-$ and $-[-PH_3)_2PtC{\equiv}CC_6H_4C{\equiv}C-]_x-$ polymers, shown in Figure 5. Only the highest occupied frontier crystal orbitals (CO) and the two lowest unoccupied C-π CO are shown in the range of −8 to −13 eV. There are several very flat bands indicating that they correspond to well localized electrons. There are two phenyl-based π-orbitals, namely those which have a zero (or small) coefficient at the α and α' carbons. These bands fall in the −13 eV to −8 eV range and carry the label π_{Ph} and π^*_{Ph}. For polyparaphenylene (PPP) or polyphenylene–vinylene (PPV) there is a pair of very flat π-bands which are analogous to our case here.[27] Further flat bands are associated with mainly M(xz) b_1, M(xy) a_2 orbitals. One of the differences between polymers

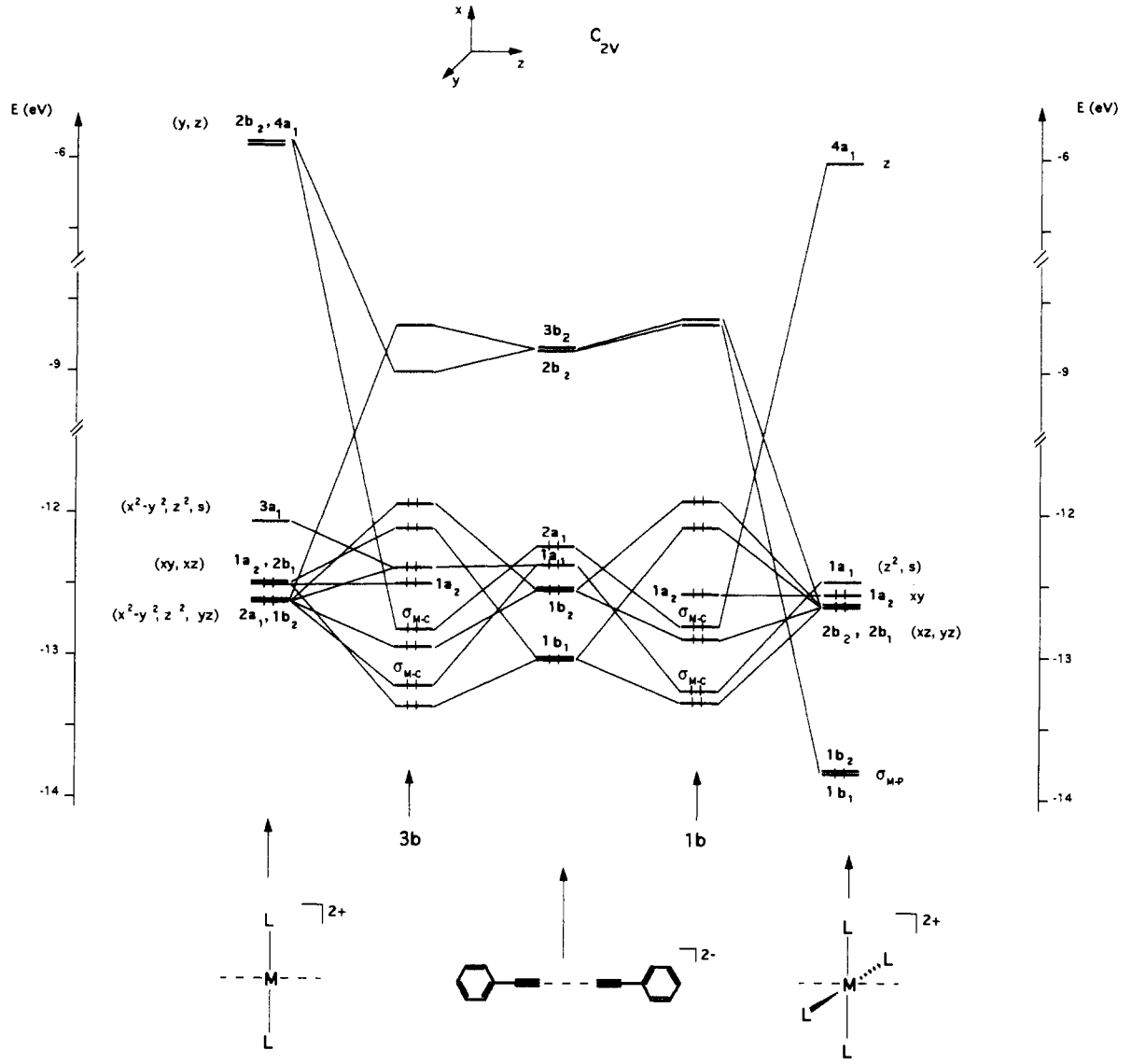

Figure 4. Interaction diagram for **3b** and **1b** (M = Fe, L = PH_3, R = *p*-C_6H_4). The principal interactions between the $[C_6H_5C{\equiv}C- - -C{\equiv}CC_6H_5]^{2-}$ and $M(L)_n^{2+}$ fragments are represented for the frontier energy levels.

Table I. Summary of Computational Results[a] for $HC{\equiv}CC_6H_4C{\equiv}CH$ (**10**), $(PH_3)_2Pt(C{\equiv}CC_6H_5)_2$ (**3b**), $Cl(PH_3)_2PtC{\equiv}CC_6H_4C{\equiv}CPt(PH_3)_2Cl$ (**3c**), and $-[-(PH_3)_2PtC{\equiv}CC_6H_4C{\equiv}C-]_x-$ (**3a**)

	11	**3b**	**3c**	**3a**[e]
HOMO[b]	−12.32	−11.95	−11.89	−11.80
LUMO[c]	−9.03	−8.74	−9.01	−9.24
gap[d]	3.29	3.21	2.88	2.56

[a] Energy in eV. [b] Highest occupied molecular orbital. [c] Lowest unoccupied molecular orbital. [d] Transition energy between the HOMO and the LUMO. [e] For polymer **3a**, the corresponding terms are HOCO, LUCO, and band gap.

1a and **3a** is in the composition of the d block: the flat band a_1 ($x^2 - y^2$) in polymer **3a** at −12.4 eV disappears in **1a** because of its interactions with two more ligands, as explained during our discussion of the molecular examples. The density of states (DOS) shows this difference, looking at the contribution of the d metal around −14.2 eV (see Figure 6a). The projections of the d metal and carbon π_y system of the density of states show the mostly metal character of the valence band near the Fermi level and the predominant carbon participation in the conduction band. The HOCO and the LUCO for both polymers **1a** and **3a** look very similar to those of the monomeric unit described previously.

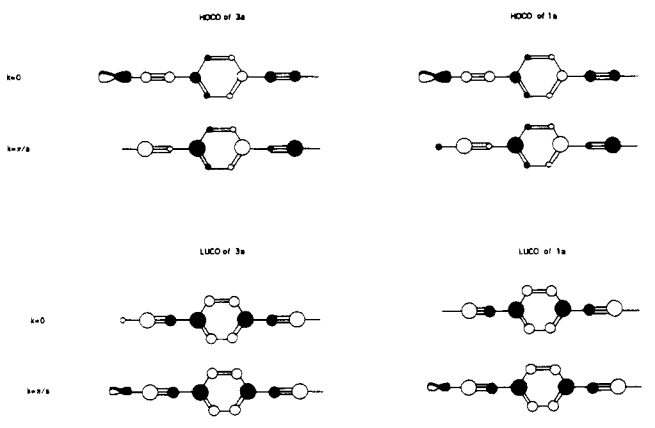

11

The HOCO and LUCO band levels are shown at the center ($k = 0$) and the edge ($k = \pi/a$) of the Brillouin zone. As discussed in the molecular section, the $M(\pi_y)$ component for the polymer **3a** stabilizes the LUCO, at $k = 0$, creating a greater conduction bandwidth than for polymer **1a**, where the $M(y)$ orbital is implicated in the σ metal–ligand bonding (see **8**, **9** and Table II). The rotation of the phenyl group by 90° for polymer **3a** moves the π system into the xz plane. Consequently, polymer **3a** in this conformation behaves similarly to the six-coordinated poly-yne **1a**, as far as the electronic properties are concerned (see Table

(27) Záliš, S.; Kertesz, M. *Synth. Met.* **1992**, *47*, 179–186.

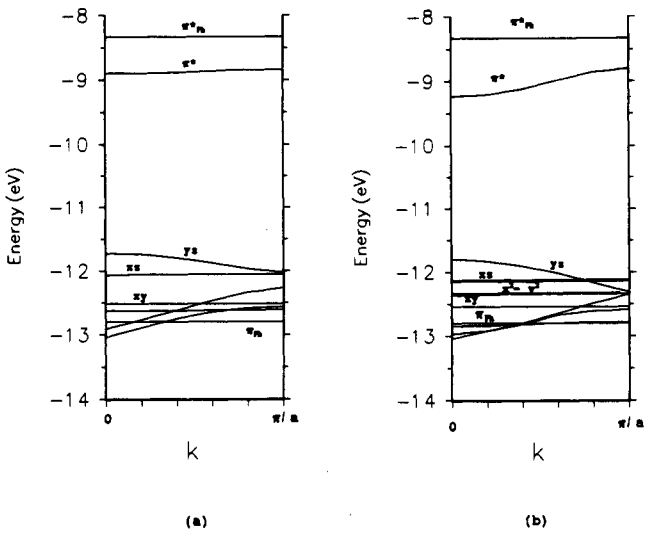

Figure 5. Band structures for metal oligo-yne polymers: (a) **1a**, $-[-(PH_3)_4FeC{\equiv}CC_6H_4C{\equiv}C-]_x-$, (b) **3a**, $-[-(PH_3)_2PtC{\equiv}CC_6H_4C{\equiv}C-]_x-$.

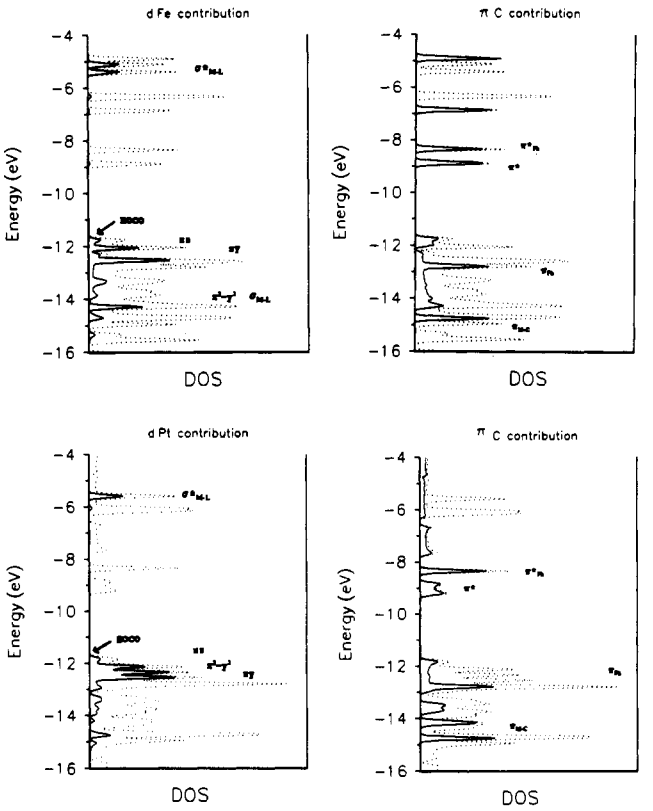

Figure 6. Density of states for metal oligo-yne polymers with the projection of the d metal orbitals (on the left) and carbon π-system (on the right) to illustrate the nature of the frontier crystal orbitals: (a, top) **1a**, $-[-(PH_3)_4FeC{\equiv}CC_6H_4C{\equiv}C-]_x-$; (b, bottom) **3a**, $-[-(PH_3)_2PtC{\equiv}CC_6H_4C{\equiv}C-]_x-$.

III). Obviously, for polymer **1a**, the rotation of the phenyl ring does not modify the electronic properties significantly because of the antibonding nature of the σ(p) orbitals, which are high in energy. In conclusion, the poly-ynes containing 4-coordinated d^8 metals **3a** have a greater conduction bandwidth by 0.4 eV than for poly-ynes containing 6-coordinated d^6 metals **1a** (see Table II). On the other hand, the dispersion of the valence band (HOCO) is in the same order (0.3–0.5 eV for **1a** (M = Fe) and **3a** (M = Pt)). At $k = 0$, the band gap value for both polymers **1a** (M = Fe) and **3a** (M = Pt) is in the 2.6–2.8-eV range, for R = *p*-C_6H_4, being in concordance with the experimentally found small conductivity. Our predicted π–π^* transitions values are in good agreement qualitatively with the experimental values of 3 eV[20,21] for poly-ynes containing platinum. We will discuss in the next section how to improve the electrical conductivity of these materials.

Table II. Summary of Computational Results[a] for the $-[-(L)_nMC{\equiv}CC_6H_4C{\equiv}C-]_x-$ Polymers (n = 2, 4; M = Ni, Pd, Pt, Rh, Co, Fe, Ru)

M	d	$(L)_n$	LUCO	CBW	HOCO	VBW	band gap
Ni	10	$(PH_3)_2$	−9.37	0.39	−12.13	0.21	2.76
Pd	10	$(PH_3)_2$	−9.14	0.22	−11.71	0.24	2.57
Pt	10	$(PH_3)_2$	−9.24	0.43	−11.80	0.51	2.56
		$(AsH_3)_2$	−9.25	0.44	−11.80	0.51	2.55
Co	9	$(PH_3)_3$, H	−8.89	0.01	−12.01	0.10	3.12
Rh	9	$(PH_3)_3$, H	−8.97	0.29	−11.47	0.24	2.50
Fe	8	$(PH_3)_4$	−8.91	0.06	−11.73	0.30	2.82
		$(CO)_4$	−8.94	0.07	−11.78	0.31	2.84
Ru	8	$(PH_3)_4$	−8.95	0.09	−12.05	0.10	3.10

[a] Energy, in eV. [b] Lowest unoccupied crystal orbital. [c] Conduction bandwidth. [d] Highest occupied crystal orbital. [e] Valence bandwidth. [f] Transition energy between the HOCO and the LUCO.

Table III. Variation of Computational Results[a] for the $-[-(PH_3)_nMC{\equiv}CC_6H_4C{\equiv}C-]_x-$ Polymers (M = Pt, Fe) with the Rotation[b] of the Phenyl Ring

θ	M	HOCO	VBW	LUCO	CBW	band gap
0	Pt	−11.80	0.51	−9.24	0.43	2.56
90	Pt	−11.80	0.35	−8.89	0.09	2.91
0	Fe	−11.73	0.30	−8.91	0.06	2.82
45	Fe	−11.73	0.30	−8.91	0.06	2.82

[a] Energy in eV. [b] Torsional angle θ in degrees. The acronyms are defined in Table II.

Table IV. Summary of the Computational Results[a] for the $-[-(PH_3)_2PtC{\equiv}CRC{\equiv}C-]_x-$ Polymers

R	none	C_6H_4	$(C{\equiv}C)_2$	$(C_6H_4)_2$	$(C{\equiv}C)_5$
LUCO	−8.92	−9.24	−9.39	−9.38	−9.64
CBW	1.19	0.43	0.51	0.23	0.21
HOCO	−11.84	−11.80	−11.81	−11.76	−11.80
VBW	0.65	0.51	0.53	0.32	0.20
band gap	2.92	2.56	2.42	2.38	2.16

[a] Energy in eV. The acronyms are defined in Table II.

The qualitative analysis of the electronic structures of the two classes of poly-yne containing transition metal indicates that (i) the delocalization of the HOCO extends over the $-M(L)_n-$ groups, for both n = 2 and n = 4 coordination and (ii) the poly-yne polymers containing 4-coordinated metal **3a** are better candidates for intrinsic doping conduction as compared to the **1a** class of 6-coordinated poly-ynes.

Band Gap as a Function of Chemical Composition

Let us extend our study of poly-ynes **1a**, **2a** and **3a** containing different transition metals M, bridging groups R, and ligands, L and X. The geometrical values are taken from the related monomeric compounds, when experimental data are available (see Table VI in the Appendix). The energetic results for the $-[-(L)_nMC{\equiv}CC_6H_4C{\equiv}C-]_x-$ and $-[-(PH_3)_2PtC{\equiv}CRC{\equiv}C-]_x-$ polymers are listed in Tables II and IV, respectively. The energy for the LUCO is for the group 10 metals lower by 0.2–0.3 eV as compared with the group 8–9 metals. The values for the corresponding LUCO bandwidths have the same trends. The energy of the HOCO is closely related to the energy of the d orbitals (see Table V in the Appendix).

We are going to describe how the electrical conductivity for poly-yne polymers could be improved, looking at the character for the HOCO and the LUCO, which determine the band gap. Concerning the HOCO, changing the nature of the metal should play some role because of the antibonding interaction between the metal and the organic chain (see **7**). The higher the energy of the d orbitals and the more diffuse they are, the higher will be the HOCO level, as illustrated in **12**. A third factor influencing the HOCO is the M-C bond distance, a short distance producing

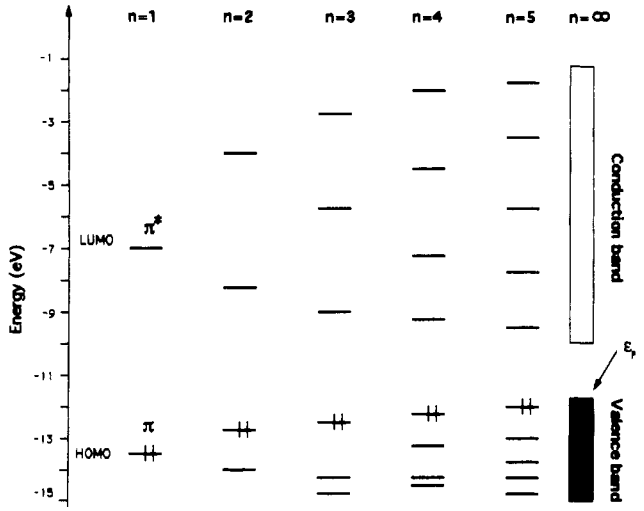

Figure 7. Relationship between the oligo-ynes $H(C{\equiv}C)_nH$ and the poly-yne $-[-C{\equiv}C-]_x-$ polymer. The solid lines represent the π molecular orbitals. The dispersions (or bandwidths) of the filled and the unfilled bands are represented by rectangles.

a higher HOCO. The final balance of these competing factors determines the HOCO level.

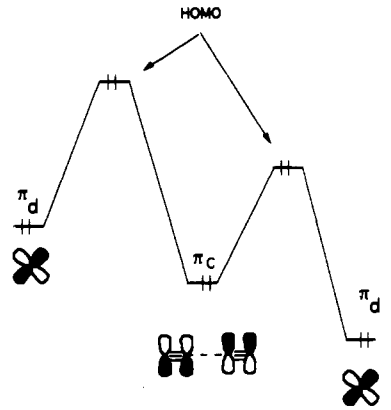

12

Even more significant concerning the conductivity of these polymers is the π-conjugation pathway of the conduction band: increasing the number of (C≡C) units in the main bridging ligand stabilizes the LUCO. Figure 7 shows the relationship between the π levels of $H(C{\equiv}C)_nH$ oligomeric acetylenes and infinite long poly-yne $-[-C{\equiv}C-]_x-$. It is clear that for a finite number of acetylide units, the LUCO value of poly-yne of −9.90 eV is reached quickly. Therefore, at our level of approximation, the energy level for the LUCO of, say, $-[-(PH_3)_2Pt(C{\equiv}C)_7-]_x-$ polymer is already very close to that of the infinite poly-yne $-[-C{\equiv}C-]_x-$ as shown in Figure 8. The value of the HOCO does not vary significantly upon the number of acetylide units, as mentioned above, the HOCO is dominated by M(d) character. Of course, the same trend is expected for poly-ynes containing metals with different coordination. In conclusion, the electrical properties for this family of polymers can be improved by changing the length of the π-system carbon backbone.

Other Coordinations and Electron Counts

Metal oligo-ynes polymers have been reported in the literature also for transition metals in coordination five[10] and two,[28,29] shown as follows:

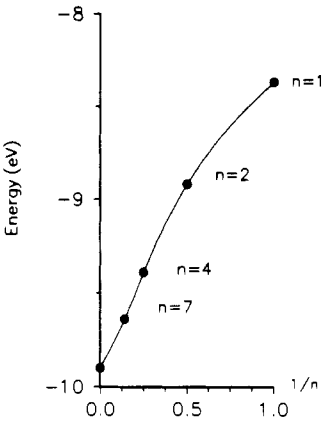

Figure 8. Correlation between the length of the oligo-yne bridging ligand $-(C{\equiv}C)_n-$ and the energy of the LUCO for the $-[-(PH_3)_2Pt(C{\equiv}C)_n-]_x-$ polymer.

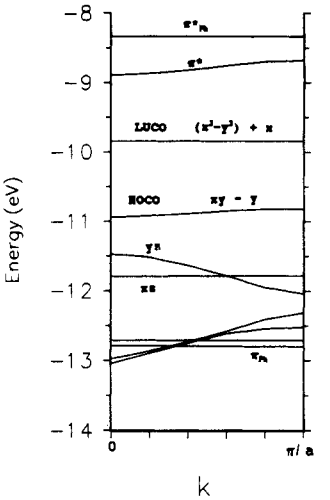

Figure 9. Band structure for $-[-(SnH_3)(PH_3)_2RhC{\equiv}CC_6H_4C{\equiv}C-]_x-$ polymer **13**.

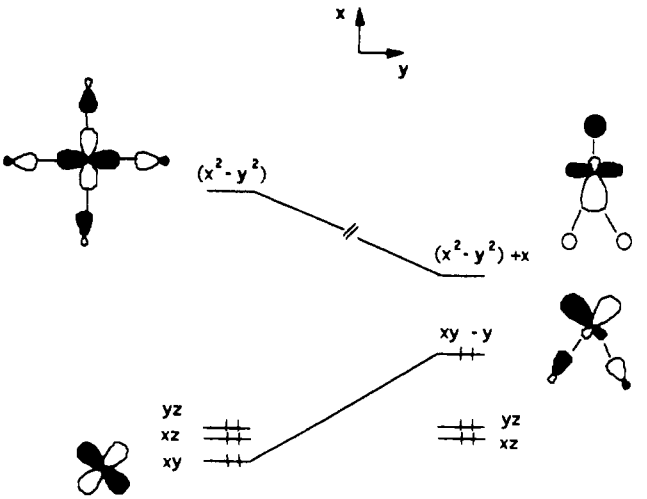

Figure 10. Orbital correlation diagram for the d orbitals which connect the octahedral and trigonal bipyramidal geometries for $(X)(L)_3M(yne)_2$ and $(X)(L)_2M(yne)_2$ molecular compounds, respectively.

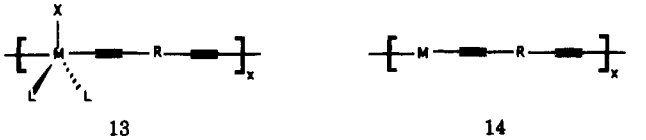

13 14

Polymer **13** is derived from polymer **2a** by removal of one phosphine ligand, giving an approximately trigonal bipyramidal configuration at each d^6 Rh^{III} metal. The band structure for the

(28) Hay, A. S. *J. Poly. Sci. Al.* **1976**, *7*, 1625.
(29) Korshak, V. V.; Sladkov, A. W.; Kurdryavtsev, Y. P. *Vysokomol. Soedin.* **1960**, *2*, 1824.

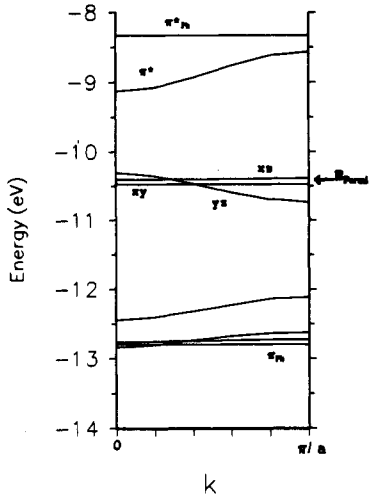

Figure 11. Band structure for $-[-(PH_3)_4MoC{\equiv}CC_6H_4C{\equiv}C-]_x-$, polymer **15**.

Table V. Orbitals Parameters Used in the Molecular and Tight-Binding EHT Calculations[a]

atom	orbital	H_{ii}, eV	ζ_1	C_1[b]	ζ_2	C_2[b]
Mo	5s	-8.34	1.96			
	5p	-5.24	1.90			
	4d	-10.50	4.54	0.6097	1.90	0.6097
Fe	4s	-9.10	1.900			
	4p	-5.32	1.900			
	3d	-12.60	5.350	0.5505	2.000	0.6260
Ru	5s	-10.40	2.080			
	5p	-6.87	2.040			
	4d	-14.90	5.380	0.5340	2.300	0.6365
Co	4s	-9.21	2.000			
	4p	-5.29	2.000			
	3d	-13.18	5.550	0.5680	2.100	0.6060
Rh	5s	-8.09	2.135			
	5p	-4.57	2.100			
	4d	-12.50	4.290	0.5807	1.970	0.5685
Ni	4s	-10.95	2.100			
	4p	-6.27	2.100			
	3d	-14.20	5.750	0.5683	2.000	0.6292
Pd	5s	-7.32	2.190			
	5p	-3.75	2.152			
	4d	-12.02	5.983	0.5535	2.613	0.6701
Pt	6s	-9.077	2.554			
	6p	-5.475	2.554			
	5d	-12.59	6.013	0.6334	2.696	0.5513
Hg	6s	-13.68	2.649			
	6p	-8.47	2.631			
	5d	-17.50	6.436	0.6438	3.032	0.5215
As	4s	-16.22	2.23			
	4p	-12.16	1.89			
P	3s	-18.60	1.880			
	3p	-12.50	1.630			
C	2s	-21.40	1.625			
	2p	-11.40	1.625			
O	2s	-32.30	2.200			
	2p	-14.80	1.975			
H	1s	-13.60	1.300			

[a] Collected by: Alvarez, S. Universidad de Barcelona, June 1989. Private Communication. [b] Coefficients in the double-ζ orbital expansion.

$-[-(SnH_3)(PH_3)_2RhC{\equiv}CC_6H_4C{\equiv}C-]_x-$ model is shown in Figure 9. In comparison with the band structure of the $-[-(L)_4FeC{\equiv}CC_6H_4C{\equiv}C-]_x-$ MOP (see Figure 5), this presents two major differences. These are interpreted using Figure 10, which shows the orbital correlation diagram for the d orbitals which connect the octahedral and trigonal bipyramidal geometries. The M(xy) level is destabilized due to its antibonding contribution to the ligand lone pairs, becoming the HOCO, for the peculiar count of 16 electrons.[10] The M(x^2-y^2) level is stabilized. This localized crystal orbital becomes the LUCO. The $\pi_M-\pi^*_M$ transition value for this polymer is only around 1 eV, with flat conduction and valence bands.

Table VI. Geometrical Parameters[a] for the MOP's and Their Related Molecular Compounds

M	M–C_{sp}	$C_{sp}{\equiv}C_{sp}$	C_{sp}–C_{sp^2}	M–M(unit cell)[b] (calcd)	ref
Mo	2.09	1.24	1.42	12.30	31
Fe	1.92	1.21	1.44	11.94	12
Ru	2.02	1.21	1.46	12.18	26c
Co	1.88	1.24	1.55	12.14	32
Rh	2.03	1.20	1.44	12.15	11
Ni	1.88	1.22	1.46	11.92	33
Pd	2.04	1.20	1.47	12.22	34
Pt	2.00	1.18	1.45	12.06	35
Hg	2.04	1.18	1.44	12.12	36

[a] Bond lengths are in angströms. [b] Distance for the repeat unit cell of $[(L)_nMC{\equiv}CPhC{\equiv}C-]_x$ polymer, in angströms. For all oligo- and polyyne models, the phenyl group and the ligands geometries are kept constant (C_{sp^2}–C_{sp^2} = 1.4 Å, C_{sp^2}–H = 1.1 Å, C_{sp^2}–C_{sp^2}–C_{sp^2} = 120°, C_{sp^2}–C_{sp^2}–H = 120°, C_{sp}–C_{sp} = 1.38 Å, M–P = 2.3–2.5 Å, P–H = 1.42 Å, M–P–H = 115°, C–O = 1.15 Å,[37] Fe–CO = 1.75 Å,[37] Rh–Sn = 2.6 Å,[38] Pt–Cl = 2.4 Å,[35] Pt–As = 2.4 Å).

Table VII. Comparison of the Experimental[a] and Modeling[b] Lengths of the Unit Cell for the Polymer Backbone Containing Platinum

unit cell	Pt–Pt dist[c]	
$-Pt(PH_3)_2C{\equiv}CC{\equiv}C-$	7.7[a]	7.74[b]
$-Pt(PH_3)_2C{\equiv}CC{\equiv}CC{\equiv}CC{\equiv}C-$	12.9	12.86
$-Pt(PH_3)_2C{\equiv}CC_6H_4C{\equiv}C-$	12.1	12.06

[a] Experimental, ref 1d. [b] Used in modeling, based on Table VI. [c] Distances in angströms.

The other MOP, $-[-HgC{\equiv}CC_6H_4C{\equiv}C-]_x-$ (**14**),[28] where d^{10} metal Hg^{II} is claimed to be in coordination 2, has also been investigated. The five M(d) levels are filled, the gap corresponds to $\pi_M-\pi^*_C$ transition of 2.60 eV. The LUCO and HOCO look like those described for **3a** (see **11**), with a smaller coefficient of the M(yz) orbital, due to the lower energy of the mercury 5d orbitals. An interesting case for MOP with the metal in coordination 2 would be the $-[-CuC{\equiv}CC_6H_4C{\equiv}C-]_x-$ polymer.[29] The electron count of 13 suggests that such a metal oligo-yne polymer containing copper, if it existed, would lead to a Peierls distortion, creating a small band gap. However, it is likely that the acetylides of neighboring chains would coordinatively bond to Hg and Cu,[30] and that the one-dimensional picture of these materials would not be a good description.

We have seen that the electron counting of 18 electrons at each d^6 metal for polymers **1a** lead to a filled d block (see Figure 4). The recently characterized deep red crystal of $(dppme)_2Mo(C{\equiv}CPH)_2$ shows a monomer of type **1b**, with a 16 electron count.[31] The band structure of the hypothetical polymer $-[-(L)_4MoC{\equiv}C_6H_4C{\equiv}C-]_x-$ (**15**) is shown in Figure 11. The polymerization of monomer **1b** containing a d^4 Mo^{II} metal by alkynyl ligand exchange[1d] might yield a corresponding polymer **1a** which could show a metallic or semimetallic character. This electron count can perhaps also be attained by oxidative doping some of the insulating MOP's discussed in this paper.

Appendix

All calculations were performed using the molecular and tight-binding extended Hückel theory.[23] The values for the H_{ii}'s and the orbital exponents are listed in Table V. For the one dimensional polymers, the electronic properties were calculated using a set of 52 K points in the Brillouin zone.

(30) Coordinative bonding of acetylides to otherwise 2-coordinated Cu are well-known. For structures of molecular examples, see e.g.: (a) Corfield, P. W. R.; Shearer, H. M. M. *Acta Crystallogr.* **1966**, *21*, 957–965. (b) Naldini, L.; Demartin, F.; Manassero, M.; Sansoni, M.; Rassu, G.; Zoroddu, M. A. *J. Organomet. Chem.* **1985**, *279*, C42. (c) Diez, J.; Gamasa, M. P.; Gimeno, J.; Aguirre, A.; Garcia-Granda, S. *Organometallics* **1991**, *10*, 1380.

(31) Buang, N. A.; Hughes, D. L.; Kashef, N.; Richards, R. L.; Pombeiro, A. J. L. *J. Organomet. Chem.* **1987**, *323*, C47–C50.

Only unit cell data exist for a few metal oligo-yne polymers.[1d,20] Therefore, we have taken the structural parameters of our models from oligo-yne monomers, whenever they were available for the metal in consideration (see Table VI). Table VII shows a good agreement between the experimental and the independent modeling values for the metal–metal distances in $-[-(L)_2\text{-}PtC{\equiv}CRC{\equiv}C-]_x-$.

Acknowledgment. G.F.'s stay at Georgetown University has been supported by the Conseil Regional de Bretagne. We thank the National Science Foundation for the generous support (Grant No. DMR9115548). We are grateful to Dr. C. X. Cui for early discussions and to John Akapulco for the drawings.

(32) Klein, H.-F.; Beck, H.; Hammerschmitt, B.; Koch, U.; Koppert, S.; Cordier, G.; Paulus, H. *Z. Naturforsch.* **1991**, *46b*, 147–156.
(33) Spofford, W. A.; Carfagna, P. D.; Amma, E. L. *Inorg. Chem.* **1967**, *6*, 1553–1557.
(34) Yasuda, T.; Kai, Y.; Yasuoka, N.; Kasai, N. *Bull. Chem. Soc. Jpn.* **1977**, *50*, 2888–2891.
(35) Cardin, C. J.; Cardin, D. J.; Lappert, M. F.; Muir, K. W. *J. Chem. Soc., Dalton Trans.* **1978**, 46–50.
(36) Gutiérrez-Puebla, E.; Vegas, A.; García-Blanco, S. *Acta Crystallogr.* **1978**, *B34*, 3382–3384.
(37) Goddard, R.; Howard, J.; Woodward, P. *J. Chem. Soc., Dalton Trans.* **1974**, 2025–2027.
(38) Bott, S. G.; Machell, J. C.; Mingos, D. M.; Watson, M. J. *J. Chem. Soc., Dalton Trans.* **1991**, 859–862.